Journal of Earthquake Engineering, 00:1–24, 2012

ISSN: 1363-2469 print / 1559-808X online
DOI: 10.1080/13632469.2012.657335

Taylor & Francis
Taylor & Francis Group

Jet-Pacs Project: Dynamic Experimental Tests and Numerical Results Obtained for a Steel Frame Equipped with Hysteretic Damped Chevron Braces

FELICE CARLO PONZO[1], ANTONIO DI CESARE[1], DOMENICO NIGRO[1], ALFONSO VULCANO[2], FABIO MAZZA[2], MAURO DOLCE[3], and CLAUDIO MORONI[3]

[1]Dipartimento di Strutture, Geotecnica, Geologia Applicata all'Ingegneria, Università della Basilicata, Potenza, Italy
[2]Dipartimento di Strutture, Università della Calabria, Rende (Cosenza), Italy
[3]Dipartimento di Protezione Civile, Roma, Italy

The experimental and numerical results obtained by Research Units of the University of Basilicata and University of Calabria for a steel frame, bare or equipped with metallic yielding hysteretic dampers (HYDs), are compared. The shaking table tests were performed at the Structural Laboratory of the University of Basilicata within a wide research program, named JETPACS ("Joint Experimental Testing on Passive and semiActive Control Systems"), which involved many Research Units working for the Research Line 7 of the ReLUIS (Italian Network of University Laboratories of Earthquake Engineering) 2005–2008 project. The project was entirely founded by the Italian Department of Civil Protection. The test structure is a 1/1.5 scaled two-story, single-bay, three-dimensional steel frame. Four HYDs, two for each story, are inserted at the top of chevron braces installed within the bays of two parallel plane frames along the test direction. The HYDs, constituted of a low-carbon U-shaped steel plate, were designed with the performance objective of limiting the inter-story drifts so that the frame yielding is prevented. Two design solutions are considered, assuming the same stiffness of the chevron braces with HYDs, but different values of both ductility demand and yield strength of the HYDs. Seven recorded accelerograms matching on average the response spectrum of Eurocode 8 for a high-risk seismic region and a medium subsoil class are considered as seismic input. The experimental results are compared with the numerical ones obtained considering an elastic-linear law for the chevron braces (in tension and compression), providing that the buckling be prevented, and the Bouc-Wen model to simulate the response of HYDs.

Keywords Shaking Table; Experimental Results; Nonlinear Dynamic Analysis; Framed Structures; Metallic Hysteretic Dampers; Performance-based Design

1. Introduction

Traditional retrofitting techniques for framed structures are based on widespread strengthening of the structure and/or on the introduction of additional, very stiff, structural members. In recent decades, innovative strategies for the passive control of structures were studied and experimented, such as those based on the insertion of damped braces, connecting two consecutive stories of the building and incorporating suitable devices,

Received 20 August 2011; accepted 10 January 2012.
Address correspondence to Fabio Mazza, Dipartimento di Strutture, Università della Calabria, Rende (Cosenza), Italy. E-mail:

purposely designed to dissipate a large amount of energy (e.g., see Soong and Dargush, 1997; Christopoulos and Filiatrault, 2006). The application to existing buildings of the energy dissipation strategy is rapidly increasing throughout the world. Several types of both passive and semi-active energy dissipating systems are in use today and many new solutions are continuously being proposed and investigated.

The dissipative bracing systems which were proposed differ for the particular arrangement of the braces and/or for the features of the dissipative device (in particular, by the way of dissipating energy). In the present work, the attention is focused on metallic yielding hysteretic dampers (HYDs), which are characterized by a stable hysteretic behavior independent on temperature and velocity of motion; their activation happens when preset stress levels are reached or overcome. These devices are generally manufactured from traditional materials and require little maintenance, representing a low cost and reliable solution for energy dissipation. The first idea of using hysteretic dampers for earthquake resistant structures was given by Kelly *et al*. [1972]. Afterwards, many HYDs were proposed in literature (e.g., see Martìnez-Rueda, 2002), but in the following only some of the most relevant worldwide applications are briefly described. The device proposed by Ciampi [1989] consists of an inner steel frame, geometrically similar to the frame mesh into which the braces are inserted, with a variable cross-section to provide uniform bending plasticization. Later, other damped steel-bracing systems where proposed and tested at the University of California at Berkeley. One of the most popular is the ADAS (Added-Damping-Added-Stiffness) damper [Whittaker *et al*., 1991], having X-shaped steel plates clamped at both ends; the tapered section of the plates allowed a uniform flexural yielding along the height of the device. Tsai *et al*. [1993] developed a variation of the ADAS system (TADAS, Triangular-Added-Damping-Added-Stiffness) using triangular steel plates, where the effect of the gravity loads is removed from the device by using slotted holes in the connection details. Moreover, E-shaped and C-shaped HYDs, whose geometry allowed an almost uniform plastic deformation, were proposed by Ciampi [1993].

A widespread diffusion of these techniques has not yet been achieved, mainly due to the lack of extensive experimental information allowing for the adoption of less conservative design rules. For this reason, an extensive dynamic experimental testing program, named JETPACS (Joint Experimental Testing on Passive and semiActive Control Systems), was carried out at the Structural Laboratory of the University of Basilicata [Dolce *et al*., 2008], within the research line No. 7 of the ReLUIS 2005–2008 executive project. The JETPACS Project has been supported by several partners from different Italian Universities, which in turn have developed or studied a number of energy dissipation devices based on different materials and/or principles. The tests have been carried out on a 1/1.5 scaled structural model derived from a 2-story, 1-bay, three-dimensional steel frame, prototype building. During dynamic testing, a total of seven different passive or semi-active energy dissipating devices based on currently available technologies (i.e., hysteretic and viscous damping) or innovative systems (i.e., shape-memory-alloy wires, magneto-rheological fluids) were used. In particular, a new type of HYD manufactured by T.I.S. S.p.A. has been studied by the Research Units of the University of Basilicata (UNIBAS) and University of Calabria (UNICAL), and presented in this work. Firstly, an overview of the experimental model set up and the detailed aspects of the experimental model, test apparatus, and sensor set up are presented. Afterwards, the efficiency of the proposed HYD in dissipating input energy and in reducing the seismic response of the structural model under moderate and strong earthquakes is investigated, in order to obtain experimental data useful for developing a design procedure. To this end, during the tests, the structural model was subjected to seven recorded accelerograms selected from ReLUIS database [Iervolino *et al*., 2008], matching on average the response spectrum of Eurocode 8 [EC8, 2003] for

a high-risk seismic region and a medium subsoil class. The seismic intensity was progressively increased, up to the attainment of the performance objective adopted in the design.

The increasing number of numerical studies on a large number of dissipative braces and the analysis of real applications have not been followed by a parallel improvement of related codes and guidelines, as in the case of other innovative techniques (e.g., seismic isolation). In Europe, new seismic codes only implicitly allow for the use of these devices (i.e., EC8, 2003; NTC, 2008), while very few codes in the world provide for simplified criteria for the design (e.g., FEMA-ASCE 356, 2000). For a widespread application of the dissipative braces, practical design procedures are needed. According to the philosophy of the *Performance-Based Earthquake Design* [Bertero, 2002], a performance design objective is obtained coupling a performance level (e.g., fully operational, operational, life safe, or near collapse) with a specific level of ground motion (e.g., frequent, occasional, rare, or very rare). Specifically, two alternative approaches can be followed: (a) the Force-Based Design (FBD) approach combined with required deformation target verification (e.g., see Kim *et al*., 2003; Ponzo *et al*., 2007b; referring to HYDs); (b) the Direct Displacement-Based Design (DDBD) approach, in which the design starts from a target deformation (e.g., see Kim and Choi, 2006; Mazza and Vulcano, 2008; referring to HYDs). A FBD procedure, aiming to proportion steel braces equipped with HYDs, in order to prevent damage to structural members, is presented in this article. Two design solutions are considered, assuming the same stiffness of the chevron braces with HYDs, but different values of both ductility demand and yield strength of the HYDs. The performance objective is expressed in terms of a threshold value of the maximum inter-story drift, lower than the yield inter-story drifts of the structure, which is supposed to respond within its elastic range during the shaking table tests. A further goal is to verify the reliability of the simplified method used to design the mechanical characteristic of the damping devices. To this end, the numerical results of nonlinear dynamic analysis carried out on the steel frame, bare or equipped with HYDs, are also reported and compared with the experimental results.

2. Experimental and Numerical Models

The experimental 1/1.5-scaled model for dynamic tests has been designed starting from a residential housing steel building prototype. Figure 1 shows a photographic view and the general layout of the experimental model. The test structure is a two-story, three-dimensional steel frame, with plan dimensions of 4 m by 3 m and inter-story height equal to 2 m. The two floors are made of HI-bond corrugated steel sheets, with upper 100 mm-thick reinforced concrete slab, connected to the primary beams. Primary and secondary beams have equal steel cross-section (IPE 180) for the two stories and the columns have constant cross-section (HEB 140) along the model height. Beam-to-column joints are welded and stiffened by horizontal plates crossing the panel zones of columns. The rigid diaphragm condition at the base of the experimental model is achieved by four steel beams (HEB 220) and two horizontal V-inverted braces (HEA 160), connected with the shaking table system of the test apparatus. Finally, four vertical V-inverted braces (HEA 100), two for each story, are inserted within the bays of two parallel frames along the test direction.

The experimental model is realized using Fe360 grade steel, having Young modulus E= 206000 N/mm^2, yielding strength f_y= 235 N/mm^2 and ultimate strength f_u= 360 N/mm^2. The gravity loads used in the design are represented by dead- and live-loads, respectively equal to 3.25 kN/m^2 and 2 kN/m^2. Four additional concrete masses have been symmetrically placed on each floor slab (see Fig. 2), to take into account the non-structural dead loads and a proper amount (30%) of live loads, as well as the contribution due to

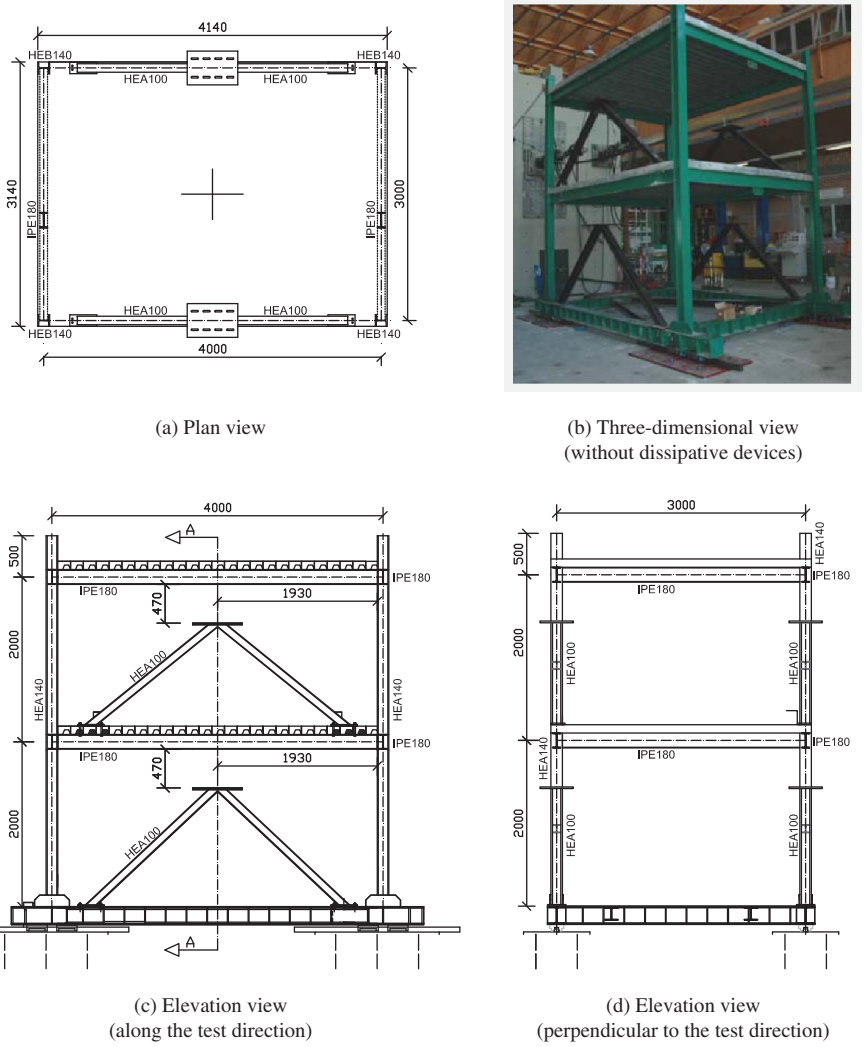

(a) Plan view

(b) Three-dimensional view (without dissipative devices)

(c) Elevation view (along the test direction)

(d) Elevation view (perpendicular to the test direction)

FIGURE 1 Experimental 1/1.5-scaled structural model (dimensions in mm) (color figure available online).

the mass-similitude scaling. The theoretical weight of the experimental model is obtained from the prototype model weight by taking the length and material scaling factors equal to 2/3 and 1, respectively. The actual total weight of the JETPACS experimental model, at the two stories, is reported in Table 1 together with model weight and additional weight.

Dynamic identification tests of the unbraced frame have been carried out at the Structural Laboratory of University of Basilicata [Ponzo *et al.*, 2007a; Serino *et al.*, 2008], by considering a number of different excitation sources: ambient noise, instrumental hammer impact excitations and sine-sweep ground motion induced by operating a nearby devices test machine. The model response has been recorded by a total of 16 uni-directional servo-accelerometers, of which 13 on the experimental model, 2 at the ground level, and 1 on the dynamic actuator. In order to obtain robust outcomes, the averaged values coming out from different only-output modal analyses techniques were considered. In Table 2, dynamic test results are reported in terms of natural periods corresponding to the translational modes along the main axes in plan (i.e., X and Y axes which are, respectively,

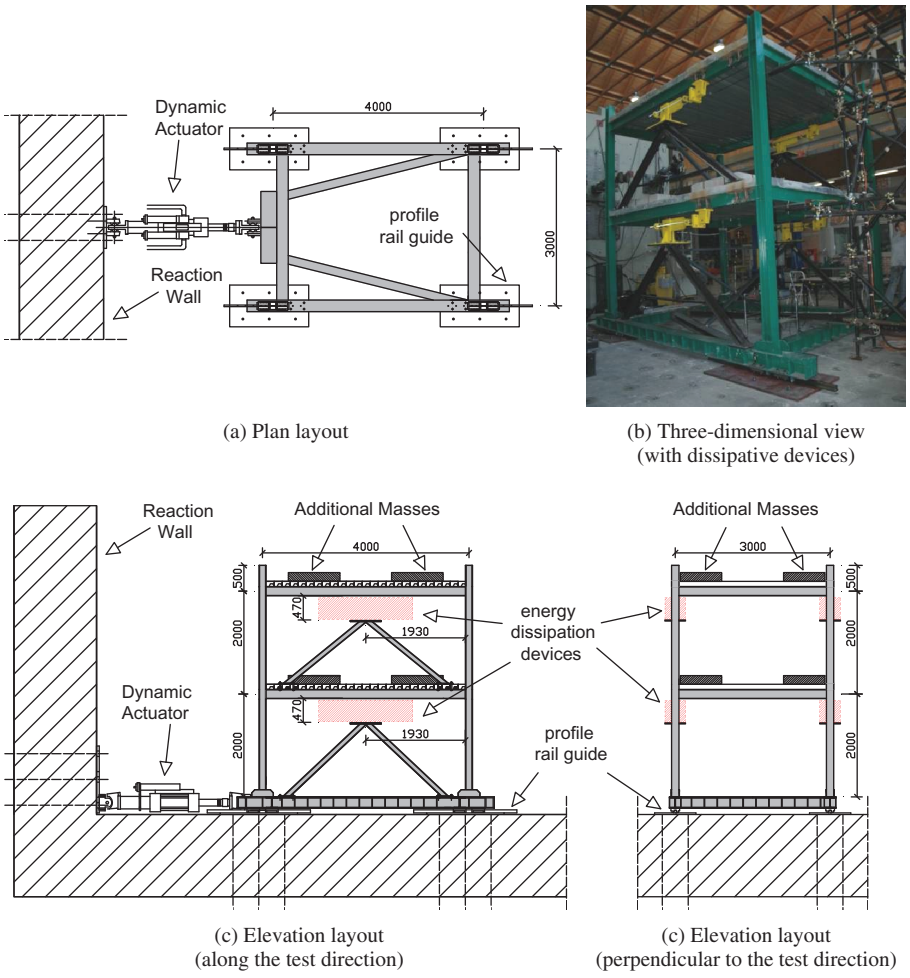

(a) Plan layout

(b) Three-dimensional view (with dissipative devices)

(c) Elevation layout (along the test direction)

(c) Elevation layout (perpendicular to the test direction)

FIGURE 2 Apparatus for dynamic tests (dimensions in mm) (color figure available online).

TABLE 1 Weight of the structural model

Story	Model weight (kN)	Additional weight (kN)	Total weight (kN)
1	36.30	13.26	49.56
2	33.35	13.20	46.55

parallel and perpendicular to the test direction) and the torsional modes around the vertical axis (i.e., Z axis). Finally, a calculation obtained from impact tests measurements [Gattulli *et al*., 2007; De Stefano *et al*., 2008; Antonacci *et al*., 2011] yields to the modal damping factor (ξ) values shown in Table 2.

The elastic-plastic devices considered in this article have been manufactured and are under patent process by T.I.S. S.p.A.. They are based on the hysteretic properties of steel plates (Fig. 3a), capable of providing the necessary additional horizontal strength, stiffness and energy dissipation capacity whilst limiting inter-story drifts. The particular technology adopted to realize these devices is constituted by low-carbon U-shaped steel plates capable

TABLE 2 Vibration periods and equivalent damping ratios of the structural model measurements [Gattulli *et al*., 2007; De Stefano *et al*., 2008]

Mode	Dominant component	T (s)	ξ (%)	Description
1	Translation along Y	0.35	0.09	In-phase displacement of the stories
2	Translation along X	0.28	0.15	In-phase displacement of the stories
3	Torsional around Z	0.19	0.07	In-phase rotation of the stories
4	Translation along Y	0.12	0.18	Counter-phase displacement of the stories
5	Translation along X	0.08	0.13	Counter-phase displacement of the stories
6	Torsional around Z	0.06	0.07	Counter-phase rotation of the stories

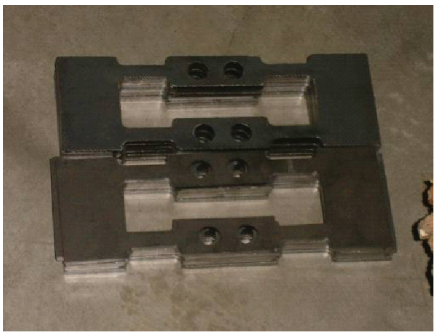

(a) View of dampers

(b) View of a damper installed on the test structure

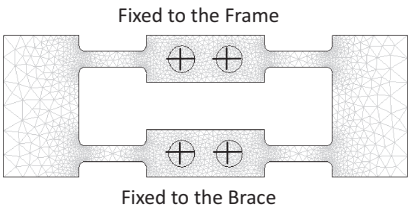

(c) Mechanism of transmission of the forces

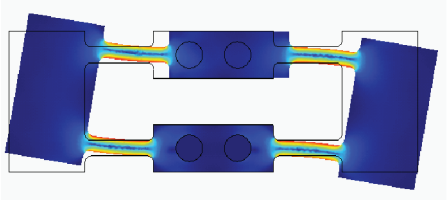

(d) Deformed shape of the plate elements

FIGURE 3 Hysteretic damper manufactured by T.I.S. S.p.A (color figure available online).

of dissipating energy by means of yielding due to flexural mechanisms during the seismic motion. The particular mechanism (Fig. 3b) allows to obtain a very large range of stiffness and strength values. Four HYDs, two for each story, are mounted on the top of two stiff steel chevron braces (HEA100), as shown in Fig. 2. Bolts ensure the rigid connection between the stiff braces and the hysteretic devices. Two additional V-inverted steel braces (UPN 80) have been realized (but not shown in Fig. 3) in the direction orthogonal to the excitation as safety system during the tests.

The test apparatus at the University of Basilicata Structural Laboratory (Fig. 2) comprises a single degree of freedom shaking table driven by a dynamic actuator, with $\pm$500kN

(a) SKF profile rail guide (b) Model base

FIGURE 4 Dynamic test apparatus at the Structural laboratory of the University of Basilicata (color figure available online).

maximum load capacity and ±250 mm stroke, fixed to a reaction wall and to the base of the test model by means of cylindrical joints (Fig. 4). The shaking table consists of a four profile rail guide system, with two carriages for each guide, located under each column of the experimental model (Fig. 4a). A friction factor of less than 1% ensures accurate linear movement in the test direction. The rigid diaphragm condition at the base level is achieved by an adequately braced steel girder (HEM 300), as shown in Fig. 4b. The model is practically a two degrees of freedom system in the test direction, corresponding to the two horizontal floors displacements, where most of the structural mass is concentrated. The actuator applied force is measured by a piezoresistive load cell mounted at the actuator end. A total of 26 acquisition channels are employed to record the structural response. The horizontal displacements of each floor are measured by 4 digital transducers fixed to an external steel reference frame. Floor accelerations are recorded utilizing a total of 8 horizontal servo-accelerometers (4 in the X-direction and 4 in the Y-direction) and 1 vertical servo-accelerometer. The table-model base accelerations are recorded by 4 horizontal servo-accelerometers (2 in the X-direction and 2 in the Y-direction) and corresponding displacements by 1 transducer also fixed to the external steel reference frame. The remaining 8 input channels are used to measure forces of the energy dissipating devices by a total of 4 piezoresistive load cells mounted at the end of each device and their relative displacement by means of 4 displacement transducers.

The steel frame has been modeled by SAP2000_Nonlinear [CSI, 2004], using frame-type finite elements (Fig. 5a) whose geometric dimensions are detailed above. The connection between the columns and the stiff beams at the base of the model has been considered. The beam-column joints of the frame (realized with stiffened full-strength welded connections) have been modeled through stiff links with length equal to half height of the corresponding beam/column. The connection between the columns and the stiff beams at the base of the model has been simulated through perfect restraints. In order to take into account a possible nonlinear behavior of the structure, suitable plastic hinges, with an axial load-dependent behavior, have been inserted at the ends of each frame element. Moreover, the in-plane behavior of the floor slabs has been captured by means of rigid diaphragm constraints. Four additional lumped masses have been symmetrically placed, on each floor slab, at the geometric coordinates of the centre of the concrete blocks shown in Fig. 2. An elastic-linear law, in tension and compression, is considered for the steel braces, providing that yielding and buckling be prevented. Finally, the nonlinear force-displacement (F_D-Δ_D) behavior of the HYDs is modeled by using link elements characterized by the Bouc-Wen monotonic (Fig. 5b) and cyclic (Fig. 5c) laws [Bouc, 1967; Wen, 1976], demonstrating a versatility in generating a variety of hysteretic patterns. More specifically, the ratio α, of

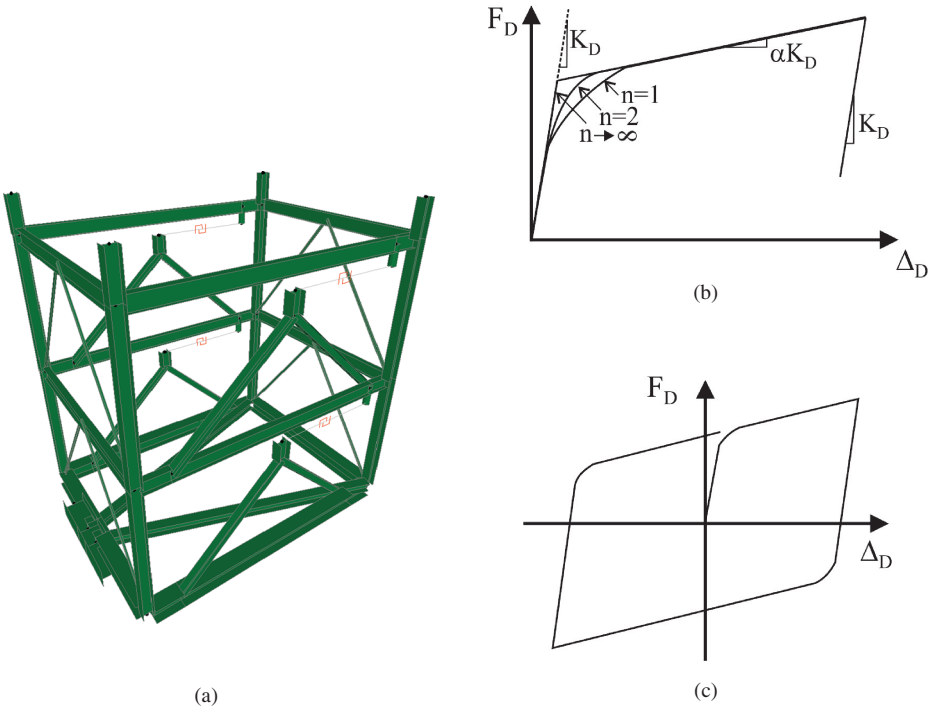

FIGURE 5 Three-dimensional finite element numerical model (a), force-displacement laws for the HYDs: Bouc-Wen monotonic (b), and cyclic (c) (color figure available online).

post-yield to pre-yield stiffness (K_D), is assumed equal to 3% while the exponent n, which regulates the shape of the hysteresis loop, is considered equal to 1.

3. Performance-based Design of the Chevron Braces with HYDs

The performance objective of the design of the chevron braces with HYDs (afterwards simply called damped braces) was to prevent damage to frame members, in such a way that the same initial conditions are guaranteed for all experimental tests and, therefore, their repeatability. Then it has been expressed as a threshold value of the maximum inter-story drift (Δ_{max}), lower than the yield inter-story drift (Δ_y) of the framed structure, whose values are showed below for both test structure stories. The framed structure, therefore, is supposed to respond within its elastic range ($\Delta_{max} < \Delta_y$) during the shaking table tests. A proportional stiffness criterion [Vulcano and Mazza, 2002], which assumes, at each story, the same value of the stiffness ratio $K^*_{DB}(=K_{DB}/K_F)$ between the lateral stiffness provided by the damped braces (K_{DB}) and that of the unbraced frame (K_F), is considered. A same value of the stiffness ratio $K^*_D(= K_D/K_F) \cong K^*_{DB}$ is obtained at the two stories, being the brace stiffness (K_B) very large in comparison with the damper stiffness (K_D). The distribution law of the yield-load (N_y) for the damping devices of the two stories is assumed similar to that of the elastic force induced in the braces by the lateral seismic loads (e.g., assuming a load distribution similar to that of the first-mode shape). Due to the above assumptions, the yield-load can be characterized at each story by a same value of the yield-ratio $N^* = N_y/N_{max}$, where N_{max} is the elastic force induced in the braces by the lateral seismic loads inducing Δ_y in a story. In the present work, two alternative design solutions

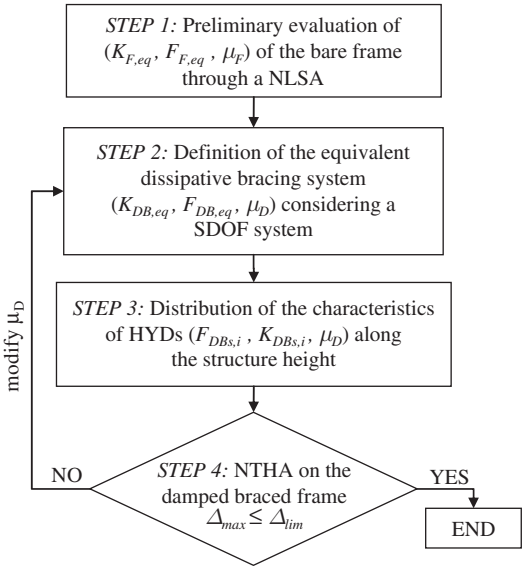

FIGURE 6 Flowchart of the design procedure.

are compared, assuming, for a same value of stiffness ratio (i.e., $K^*_{DB}=2$), different values of yield-ratio (N^*) and ductility demand (μ_D) of the HYDs: the first design solution, proposed by the University of Basilicata (labeled as Type1_UNIBAS), provides $N^*=0.05$ and $\mu_D=10$, while on the basis of the second design solution, proposed by the University of Calabria (labeled as Type2_UNICAL), $N^*=0.10$ and $\mu_D=5$ are assumed.

The main steps of the iterative procedure, as better detailed in Ponzo *et al*. (2007b), are summarized below (see flowchart in Fig. 6).

The first step of the design procedure consists in a preliminary evaluation of the unstrengthened steel frame lateral resistance in the test direction, through a nonlinear static analysis (NLSA) carried out considering, besides the gravity loads, two distributions of the horizontal forces: one proportional to the masses ("rectangular") and the other one related to the first modal shape (practically, "triangular"), both applied in the center of masses of each floor. The results of nonlinear static analysis are shown in Fig. 7a in terms of normalized values of base shear (base shear/model weight ratio) and roof displacement (roof displacement/model height ratio).

As can be seen in Fig. 7a, the roof drift index (i.e., the top displacement divided by the total height of the structure) related to the onset of yielding is equal to about 0.7%. Correspondently, maximum inter-story drifts (i.e., inter-story displacements divided by the clear height of the columns) of about 0.75% are found at both stories. Then, the hysteretic dissipative braces have been designed with the main objective of limiting the maximum inter-story drifts under the yield drift obtained assuming the peak ground acceleration (PGA=0.35 g x 1.25=0.44 g) for high-risk seismic zone (a_g=0.35 g) and medium subsoil class (subsoil parameter for ground type B, S=1.25). A target drift of 0.5% is obtained considering a Safety Factor (SF) equal to 1.5.

In the second step, starting from the smallest lateral resistance curve (in the examined case that corresponding to the triangular distribution load shown in Fig. 7a), reduced according to the transformation factor Γ of the first modal shape, the equivalent bilinear single-degree-of-freedom (SDOF) system has been found. The mechanical characteristics of the equivalent bracing system are determined by the iterative procedure illustrated below

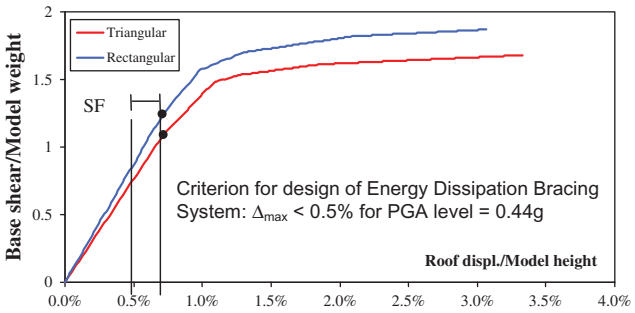

(a) Capacity curves and yield points of the test structure

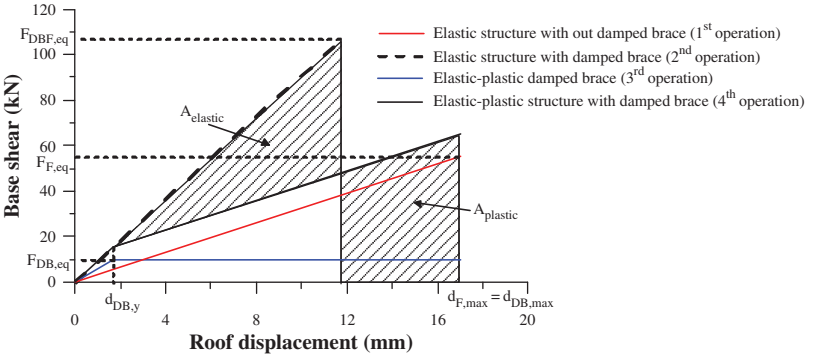

(b) Type1_UNIBAS ($\mu_D = 10$, $N^* = 0.10$)

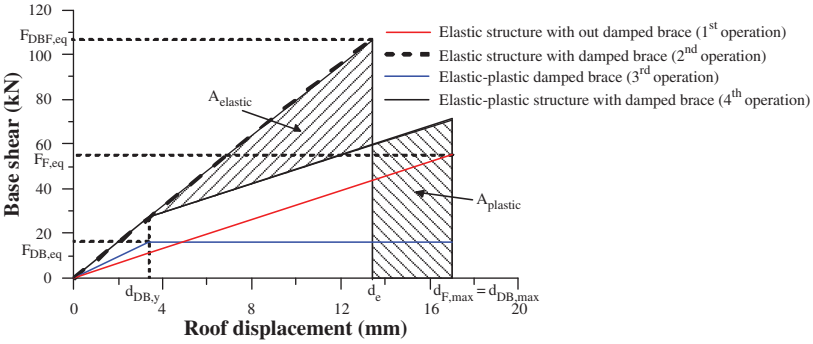

(c) Type2_UNICAL ($\mu_D = 5$, $N^* = 0.05$)

FIGURE 7 Capacity curves (a) and design of the HYDs according to the equal energy criterion (b, c) (color figure available online).

with reference to the design solutions Type1_UNIBAS and Type2_UNICAL shown in Figs. 7b and c, respectively:

1. a first hypothetical ductility value for the equivalent dissipating brace ($\mu_{DB} \cong \mu_D$ for $K^*_{DB} \cong K^*_D$) is assumed, consistent with the properties of the considered HYD. Such initial value is assumed equal to 10 or 5 by the Research Units of UNIBAS or UNICAL, respectively. Typically, the ductility of devices based on steel yielding can reach higher values, greater than 20, with good stability of behaviour for an adequate number of cycles [Dolce *et al.*, 1996];

2. the seismic force at j-th step ($F_{DBF,eq}^{(j)}$) for the equivalent elastic single-degree-of-freedom (SDOF) system is evaluated, as a function of the global dynamic characteristics of the braced structure and of the design earthquake; the initial value of the design force ($F_{DBF,eq}^{(0)}$) is obtained multiplying the equivalent mass of the model (m^*) by the pseudo-acceleration $S_e(T^*)$ derived from the elastic response spectrum for the equivalent period of the structure without damped braces (T^*_F);
3. the yield displacement of the equivalent bilinear brace ($d_{DB,y}$) is determined, starting from the available ductility μ_{DB} fixed at step 1 and imposing that the maximum displacement of the equivalent damped brace ($d_{DB,max}$) is equal to the elastic target displacement of the equivalent unbraced structure ($d_{F,max}$). The yielding force of the equivalent damped brace ($F_{DB,eq}$) is determined by means of the "equal energy criterion," considering the equivalent elastic SDOF system and the equivalent elastic-plastic SDOF system of the damped braced structure.

By step 2 it is possible to calculate the yield force of the equivalent elastic-plastic brace at j-th step ($F_{DB,eq}^{(j)}$), which allows one to determine the stiffness of the equivalent damped brace ($K_{DB,eq}^{(j)}$), the vibration period of the damped braced frame ($T^*_{DBF,j}$), and a new value of the seismic elastic force ($F_{DBF,eq}^{(j+1)}$). The procedure converges to solution when the difference between the elastic seismic forces evaluated in two consecutive loops is less than an acceptable tolerance.

The mechanical characteristics of the single device along the height of the model are evaluated in the third step. The stiffness distribution of the equivalent elastic-plastic device (representing the story devices as a whole) is made under the hypothesis that the ratio between the equivalent bracing stiffness ($K_{DB,i}$) and the stiffness of the unbraced structure ($K_{F,i}$), at the i-th story, is equal to the ratio between the stiffness of the equivalent damped brace ($K_{DB,eq}$) and the stiffness of the equivalent elastic system of the unbraced structure ($K_{F,eq}$):

$$\frac{K_{DB,i}}{K_{F,i}} = \frac{K_{DB,eq}}{K_{F,eq}} \qquad \rightarrow \qquad K_{DB,i} = K_{F,i}\frac{K_{DB,eq}}{K_{F,eq}}. \tag{3.1a,b}$$

With regard to the strength distribution at the i-th story, the ratio between the equivalent bracing strength ($F_{DB,i}$) and the strength of the unbraced structure ($F_{F,i}$) is assumed equal to the ratio between the strength of the equivalent damped brace ($F_{DB,eq}$) and strength of the equivalent elastic system of the primary structure ($F_{F,eq}$) corresponding to the yield displacement ($d_{F,y}$):

$$\frac{F_{DB,i}}{F_{F,i}} = \frac{F_{DB,eq}}{F_{F,eq}} \qquad \rightarrow \qquad F_{DB,i} = F_{F,i}\frac{F_{DB,eq}}{F_{F,eq}}. \tag{3.2a,b}$$

The distribution laws of stiffness Eq. (3.1a,b) and strength Eq. (3.2a,b) along the building height have been obtained combining, respectively, the hypothesis of a constant value of the stiffness ratio $K^*_{DB}(=K_{DB}/K_F)$ and yield-ratio $N^*(=N_y/N_{max})$, at each story, with the assumption of an equivalent single-degree-of-freedom system representing the actual damped structure. The stiffness $K_{F,i}$ and strength $F_{y,i}$ of i-th story of the primary structure are determined through a linear static analysis. Stiffness and strength of the equivalent i-th story device are distributed among the single devices ($K_{DBs,i}$ and $F_{DBs,i}$) proportionally for the two-story devices.

The mechanical characteristics of the HYDs, obtained by the iterative aforesaid procedure, are summarized in Table 3. The actual experimental values of $F_{DBs,i}$ have been

TABLE 3 Mechanical characteristics of the hysteretic damped braces

		$F_{DBs,i}$ (kN)		$K_{DBs,i}$ (kN/mm)		
Design solutions	Level	Experimental values	Design values	Experimental values	Design values	$\mu_{D,i}$
Type1_UNIBAS	I	7.5	5.0	7.0	7.0	10
	II	4.5	3.5	4.0	4.0	10
Type2_UNICAL	I	10.0	8.0	7.0	7.0	5
	II	7.0	5.5	4.0	4.0	5

assumed higher than the design values in order to take into account of the industrial standardization in the production of the devices.

The design procedure considered to evaluate the mechanical characteristics of the devices maximizes the value of energy dissipated by the device with an acceptable value of ductility demand and provides a lower bound over which the maximum acceleration and drift become constants [Ponzo and Di Cesare, 2009]. The effectivness of the proposed design procedure has been verified only with reference to cases in which the structural response is not severely affected by higher mode effects due to high-rise buildings. According to the proportional stiffness criterion, it can be reasonably assumed that a mode shape of the primary frame remains practically the same even after the insertion of damped braces. Therefore, this design criterion is preferable in the case of a retrofitting, because the stress distribution of the framed structure remains practically unchanged. Moreover, an improvement of the procedure for in-plan irregular buildings has been recently proposed by Di Cesare *et al*. [2011].

4. Seismic Input

To evaluate the effects induced by the damped braces on the seismic response of the test structure, many experimental and numerical nonlinear dynamic analyses have been carried out considering real ground motions. Specifically, seven recorded accelerograms, available in the *European Strong Motions* database (www.reluis.it) and considered in ReLUIS project, were selected taking into account the assumptions made, with regard to seismic intensity (seismic zone 1, a_g=0.35 g) and ground type (subsoil class B, subsoil parameter S=1.25), in the design of the experimental model (i.e., PGA=1.25x0.35 g=0.44 g). The corresponding main data are reported in Table 4, i.e., station, identification number of the registration, magnitude, peak ground acceleration (PGA) in the horizontal direction, and scale factor (SF) suggested by Iervolino *et al*. [2008].

The pseudo-acceleration (elastic) response spectra of the seven accelerograms match, on average, EC8 spectrum for a subsoil class B, in the range of periods 0.05–2 s. The displacement and pseudo-acceleration (elastic) response spectra of the seven accelerograms are shown in Figs. 8a and b, respectively, together with the corresponding medium spectrum and EC8 spectrum, assuming an equivalent viscous damping ratio ξ=5%. To ensure consistency with the scale of the model, all accelerograms are then scaled down in time by the factor $(1.5)^{1/2}$.

The experimental program was developed in 18 and 21 seismic tests, respectively, for UNIBAS and UNICAL research units. The intensities of the ground motions (expressed as percentage of the peak ground accelerations: PGA%) which were assumed for the

TABLE 4 Characteristics of the recorded ground motions (European Strong Motion database)

Earthquakes	Station	Registration	Magnitude	PGA/g	SF
Izmit (Turkey), 17/08/1999	Gezbe-Tubitak	001228xa	7.6	0.357	1.0
Montenegro (Serbia), 15/04/1979	Petrovac Hotel Oliva	000196xa	6.9	0.454	1.0
Erzican (Turkey), 13/03/1992	Erzican-Mudurlugu	000535ya	6.6	0.769	1.5
Tabas (Iran), 16/09/1978	Tabas	000187xa	7.3	0.926	1.5
Campano-Lucano (Italy), 23/11/1980	Calitri	000291ya	6.9	0.264	1.5
South Iceland (Iceland), 17/06/2000	Hella	004673ya	6.5	0.716	1.5
South Iceland (Iceland), 17/06/2000	Selsund	004673ya	6.5	0.716	1.0

experimental and numerical tests are summarized in Table 5 with reference to the selected accelerograms.

During testing of the model equipped with energy dissipation systems, the seismic inputs have been applied at increasing amplitudes, i.e. increasing levels expressed in percentage of the peak ground acceleration (10%, 25%, 50%, 75%, 100%, and 125%), up to a maximum value corresponding to the fulfillment of the design performance criterion (i.e., a limit value of the inter-story drifts, Δ_{max}=0.5%, to avoid yielding of the frame members and guarantee repeatability of the test). Three ground motions (namely 1228xa, 196xa, and 535ya) were scaled at different amplitudes, with PGA fractions ranging from 10–125%. The corresponding displacement and pseudo-acceleration (elastic) response spectra are shown in Figs. 8c and d, respectively. As can be observed in Fig. 8d, medium pseudo-acceleration response spectrum fits well EC8 response spectrum. More specifically, only the UNICAL experimental tests Nos. 20 and 21 were carried out up to the highest seismic intensity (i.e., PGA%=125%) of these motions, according to the above mentioned performance criterion. The remaining four natural motions were applied at 75%, 100%, and 125% of their original amplitudes. More specifically, only the UNIBAS experimental test No. 18 and UNICAL experimental tests Nos. 18 and 19 were carried out up to the seismic intensity PGA%=100%, while the highest seismic intensity (i.e., PGA%=125%) is resulted not consistent with the performance criterion.

In order to check the reliability of the shaking table response a procedure of normalization of the output signal was applied at the end of each test. The normalized value of the table peak acceleration (NPA) is then obtained by equating the Housner intensities of the original signal (input) and the filtered table signal (output) by: NPA = (HIoutput/HIinput) PGAinput. This consisted of the cleaning of the output-signal with a 30 Hz lowpass filter and then on the normalization of the maximum acceleration based on the Housner intensity calculated in the range of periods between 0.15 and 2.0 s. The Housner intensity (HI) is defined as the integral of the pseudo-velocity response spectrum calculated in a proper period range, obviously including the fundamental period of the structure.

In Fig. 8c, the NPA values are reported as a function of the table PGA, for all the dynamic tests. The NPA values are almost equal to the peak acceleration of the input

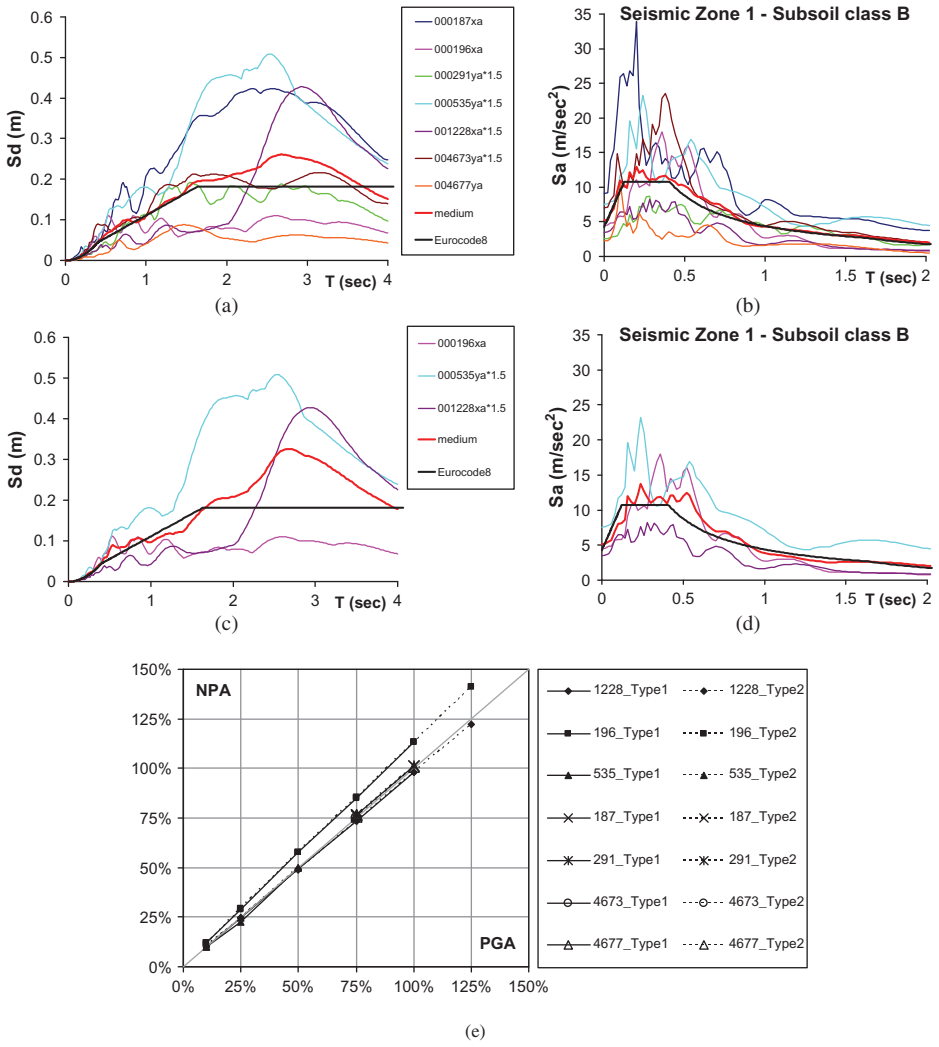

FIGURE 8 Displacement (a,c) and pseudo-acceleration (b,d) elastic response spectra corresponding to the scaled accelerograms. Comparison between NPA and PGA for all tests of Type1 and Type2 dissipative solutions (e) (color figure available online).

(PGA), with exception of the earthquake 196. In this case a constant amplification of 10% is observed for all the intensities, which did not alter significantly the correctness of the testing results.

5. Experimental and Numerical Results

In order to check the effectiveness of the damped braces when using the two considered design solutions above described (afterwards labelled as Type1_UNIBAS and Type2_UNICAL), extensive shaking table tests have been carried out at the Structural Laboratory of the University of Basilicata assuming different intensities of the selected accelerograms, in terms of the peak ground acceleration in percent (see PGA% in Table 5). As a comparison, the response of the bare structure (without Energy Dissipation Braces:

TABLE 5 Summary of the experimental tests carried out assuming different intensities of the selected accelerograms (in terms of the peak ground accelerations in percent: PGA%)

PGA %	001228xa	000196xa	000535ya	000187xa	000291ya	004673ya	004677ya
(a) Type1 UNIBAS research unit							
125	–	–	–	–	–	–	–
100	16	17	–	18	–	–	–
75	10	11	–	12	13	14	15
50	7	8	9	–	–	–	–
25	4	5	6	–	–	–	–
10	1	2	3	–	–	–	–
(b) Type2 UNICAL research unit							
125	20	21	–	–	–	–	–
100	16	17	–	–	18	–	19
75	10	11	–	12	13	14	15
50	7	8	9	–	–	–	–
25	4	5	6	–	–	–	–
10	1	2	3	–	–	–	–

w/o EDB's) has been also evaluated with regard to the lowest levels of seismic intensity (i.e., PGA%=10% and 25%) of the seven selected accelerograms, so avoiding damage of the frame members.

At first, time histories of drift at the two floor levels of the test structures are shown in Fig. 9 for the experimental test No. 5, which corresponds to the accelerogram 196 and to a level of seismic intensity (i.e., PGA%=25%), preventing the occurrence of yielding of the bare structure. As can be observed, the bare structure shows values of the drift at the second level (in Fig. 9b, $\Delta_{max,II} \cong 0.5\%$) higher than those recorded at the first level (in Fig. 9a, $\Delta_{max,I} \cong 0.35\%$). On the other hand, Type1_UNIBAS and Type2_UNICAL structures provide comparable results, ensuring a remarkable reduction of the response also for such a level of seismic intensity which corresponds to the achievement of the limit state of damage for the bare structure. More specifically, a reduction of the maximum drift above the 100%, in comparison with that of the bare structure, and a comparable response at both the floor levels can be pointed out. Finally, the force-displacement laws for the hysteretic dampers of Type1_UNIBAS and Type2_UNICAL structures (only a damper for each level is considered according to the symmetry in plan) highlight a comparable behavior (Fig. 10).

Curves analogous to those just shown are reported in Figs. 11 and 12, referring to the accelerogram 196 for the level of seismic intensity equal to 100%. The comparison is restricted to the damped braced structures, because the test on the bare structure has been not executed expecting damage of the frame members. Time histories of drift at the two floor levels exhibit a similar trend, with a maximum value of about 0.4%, which is comparable with the maximum values previously observed for the bare structure subjected to the accelerogram E-mail: 196@25%. Moreover, Type1_UNIBAS and Type2_UNICAL structures have analogous responses in terms of drift (Fig. 11) and a stable hysteretic behaviour with a large damping capacity as regards the force-displacement laws of the hysteretic dampers (Fig. 12), confirming reliability and effectiveness of the retrofitting technique even changing the design solution.

Afterwards, the maximum inter-story drift (Fig.13a) and the maximum load attained by the damper at the first story (Fig. 13b), both measured for the two design solutions, are

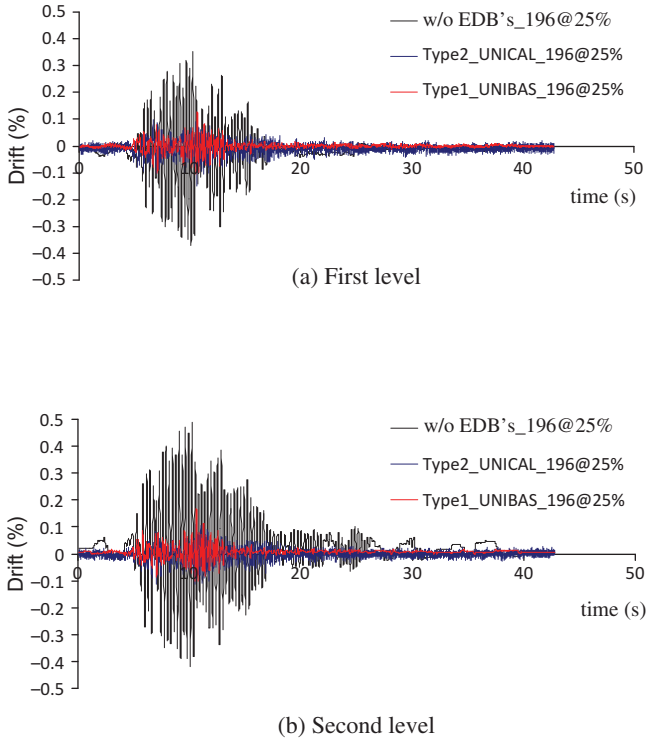

(a) First level

(b) Second level

FIGURE 9 Time histories of drift at the two floor levels: 196@25% accelerogram (color figure available online).

compared considering the accelerogram 196 at different levels of seismic intensity (i.e., 25%, 50%, 75%, and 100%). As can be seen, for each intensity of the ground motion, the adoption of Type2_UNICAL led to drifts lightly less than the corresponding ones experienced using Type1_UNIBAS. However, as expected, the maximum load reached by the device was greater for Type2_UNICAL; this led to slightly higher values of the floor accelerations, which are omitted for sake of brevity.

Finally, the mean values of the maximum inter-story drifts and the maximum load attained by the devices at the two stories, obtained on the basis of experimental and/or numerical results with reference to the selected seven accelerograms, are shown in Fig. 14. Conclusions analogous to those drawn above with reference to Fig. 13 follow also from the last results. It is interesting to note that the values of the mean inter-story drifts at both the stories (Fig. 14a) are comparable (this means an optimal activation of the dampers) and, in all the cases, not much less than (or about) the target value of 0.5%.

A collection of experimental results in terms of maximum values of inter-story drift, acceleration at the floor levels (divided by the gravity acceleration) and damper force at the first level are reported in Fig. 15 for different accelerograms and seismic intensities. More precisely, shaking table tests corresponding to all accelerograms are compared for PGA% intensities of 25%, 50%, 75%, and 100%. Seismic response of the bare structure within PGA% equal to 25% is also plotted. For all the examined levels of PGA%, Type1_UNIBAS and Type2_UNICAL structures exhibit the highest values of drift (Fig. 15a) and acceleration (Fig. 15b) when subjected to the accelerogram 535 (for 50% of PGA), unlike the bare structure having the maximum effects when subjected to the accelerogram E-mail: 196@25%. This behavior can be explained comparing the acceleration (elastic)

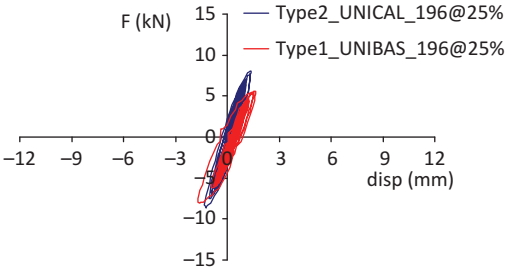

(a) First level

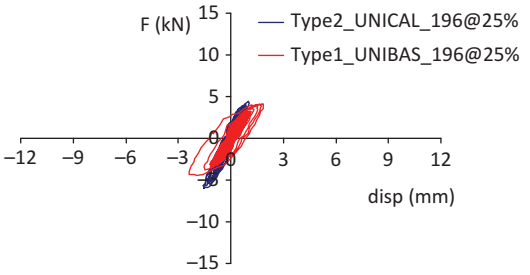

(b) Second level

FIGURE 10 Force-displacement law for the hysteretic dampers: 196@25% accelerogram (color figure available online).

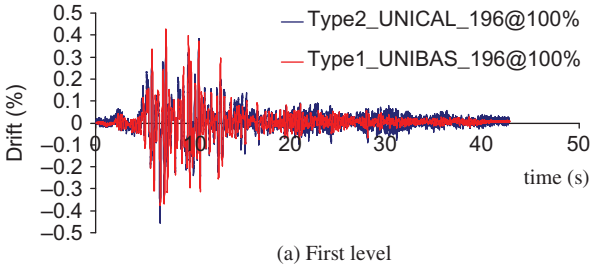

(a) First level

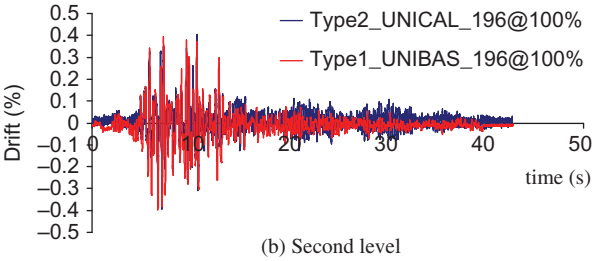

(b) Second level

FIGURE 11 Time histories of drift at the two floor levels: accelerogram 196@100% (color figure available online).

response spectra of these ground motions reported in Fig. 8 and evaluating the spectral values corresponding to the fundamental vibration periods of the structure with 430
($T_{1,DBF} \cong 0.16$ s) and without (see Table 2) damped braces. Moreover, Type1_UNIBAS and Type2_UNICAL structures provide similar responses and highlight a very good behavior also considering the accelerogram E-mail: 535@50%, which is characterized by spectral

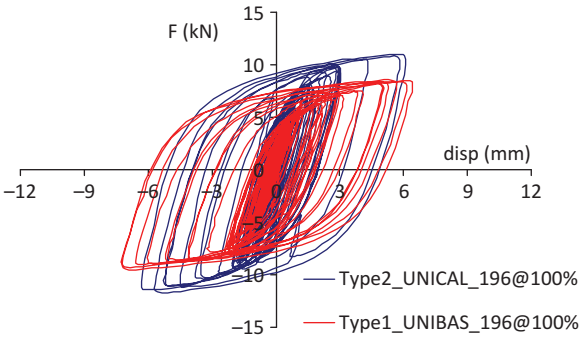

(a) First level

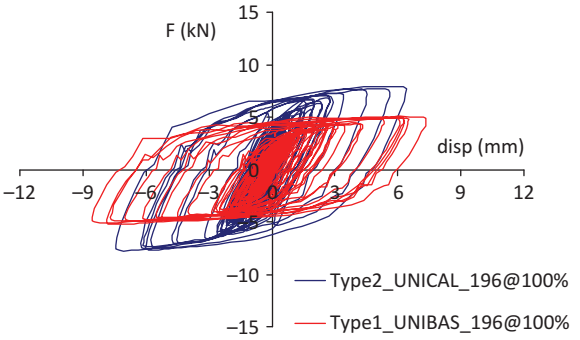

(b) Second level

FIGURE 12 Force-displacement laws for the hysteretic damper: accelerogram 196@ 100% (color figure available online).

values very high in comparison with those of the elastic design spectrum in the range of vibration periods of interest for the examined cases ($T_1 \leq 0.277$ s).

Moreover, Table 6 shows the ductility demand during the experimental tests for both dissipative systems. It can be seen that the ductility demand is, on the average, approximately equal to the design value (calculated for an intensity equal to 100% of PGA).

Finally, a comparison between experimental and numerical results for both design solutions is presented in Figs.16, 17, and 18, where the curves were obtained with reference to the accelerogram E-mail: 196@100% (i.e., test no. 17 in Table 5). More specifically, the curves represent the inter-story drifts (Fig. 16), the floor accelerations (Fig. 17), and the force-displacement laws for the hysteretic damper (Fig. 18) at each structural level for both the design solutions (i.e., Type1_UNIBAS and Type2_UNICAL). As shown, the numerical model is capable of simulating adequately the observed experimental behaviour, representing a reliable tool for predicting the nonlinear seismic response. The above results show also that the responses of the structures with different values of the strength (but a same stiffness) of the hysteretic damped braces are comparable. This behavior further proves the reliability and robustness of the design procedure, as already shown in Ponzo and Di Cesare [2009].

6. Conclusions

An extensive program of shaking table tests, on a 1/1.5-scale model of a two-story, three-dimensional steel frame, has been carried out at the Structural Laboratory of the University

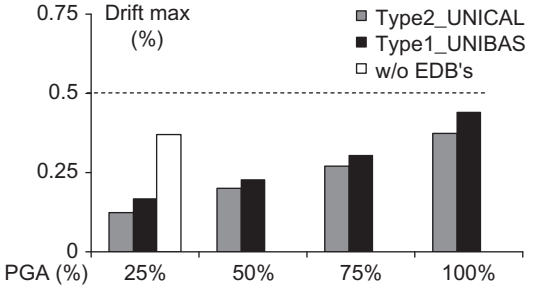

(a) Maximum inter-story drift

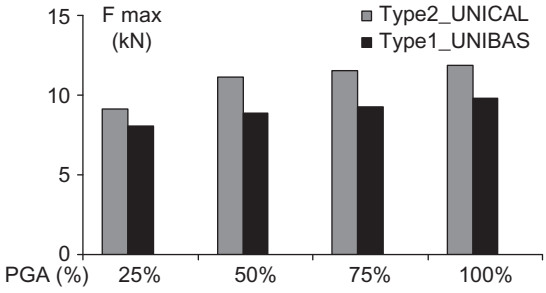

(b) Maximum load attained by the damper at the first story

FIGURE 13 Comparison between maximum values obtained from the experimental results using Type1_UNIBAS and Type2_UNICAL structures subjected to the accelerogram 196 at different levels of seismic intensity.

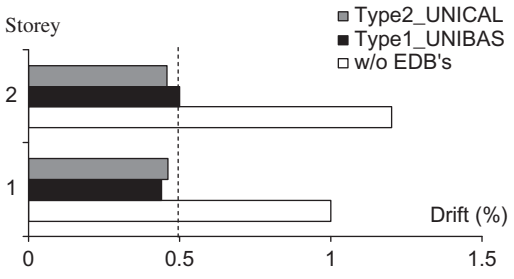

(a) Maximum inter-story drift

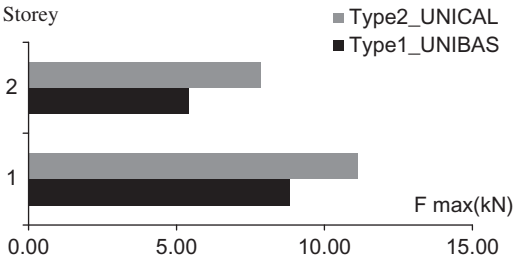

(b) Maximum load attained by the damper at the first story

FIGURE 14 Comparison between mean values obtained from the experimental and/or numerical results using Type1_UNIBAS and Type2_UNICAL structures subjected to the set of seven accelerogram in Table V (PGA100%).

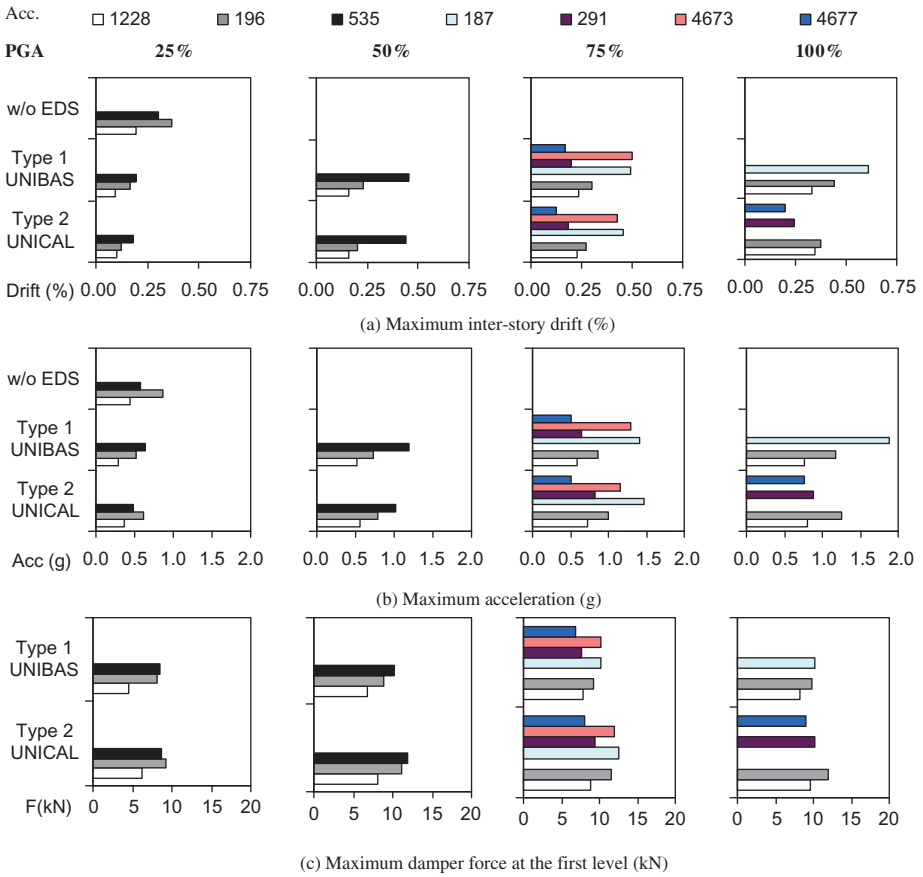

FIGURE 15 Comparison between experimental results considering different ground motions and seismic intensities: all accelerograms for PGA% intensities of 25%, 50%, 75%, and 100% (color figure available online).

of Basilicata. In particular, a new type of HYD manufactured by T.I.S. S.p.A. has been studied by the Research Units of the University of Basilicata (UNIBAS) and University of Calabria (UNICAL). During testing of the model equipped with EDB systems, the seismic inputs have been applied at increasing amplitudes, i.e., increasing levels expressed in percentage of the peak ground acceleration, up to a maximum value corresponding to the attainment of the design performance criterion (i.e., a limit value of the inter-story drifts to avoid yielding of the frame members and guarantee repeatability of the test).

In the present work two design solutions (i.e., Type1_UNIBAS and Type2_UNICAL) have been considered, assuming the same stiffness, but different values of both ductility demand and yield strength of the HYDs. The experimental results are compared with the numerical ones. A good agreement between experimental and numerical results is observed; moreover, the effectiveness of the hysteretic EDB system in reducing seismic effects, if compared to that of the structure without EDB, and the reliability of the design procedure are proved. In fact, the seismic response of the model with this EDB system shows a maximum inter-story drift, at high seismic intensities, which is smaller than the established yield limit, achieving an average reduction of the inter-story drift of the order of 2.5–3 times. Both the design solutions led to a comparable level of protection for the framed

TABLE 6 Summary of the experimental ductility demand of HYDs assuming different intensities of the selected accelerograms (in terms of the peak ground accelerations in percent: PGA%)

%	001228xa	000196xa	000535ya	000187xa	000291ya	004673ya	004677ya
(a) Type1_UNIBAS ($\mu_D = 10$)							
125	–	–	–	–	–	–	–
100	6.2	8.9	–	11.4	–	–	–
75	4.4	5.7	–	9.1	3.7	9.4	3.1
50	2.9	4.2	8.5	–	–	–	–
25	1.8	2.4	3.7	–	–	–	–
10	1.0	1.5	1.0	–	–	–	–
(b) Type2_UNICAL ($\mu_D = 5$)							
125	6.4	6.4	–	–	–	–	–
100	4.8	5.2	–	–	3.4	–	2.8
75	3.2	3. 8	–	6.4	2.6	6.0	1.7
50	2.2	2.8	6.1	–	–	–	–
25	1.4	1.7	2.5	–	–	–	–
10	1.0	1.2	1.0	–	–	–	–

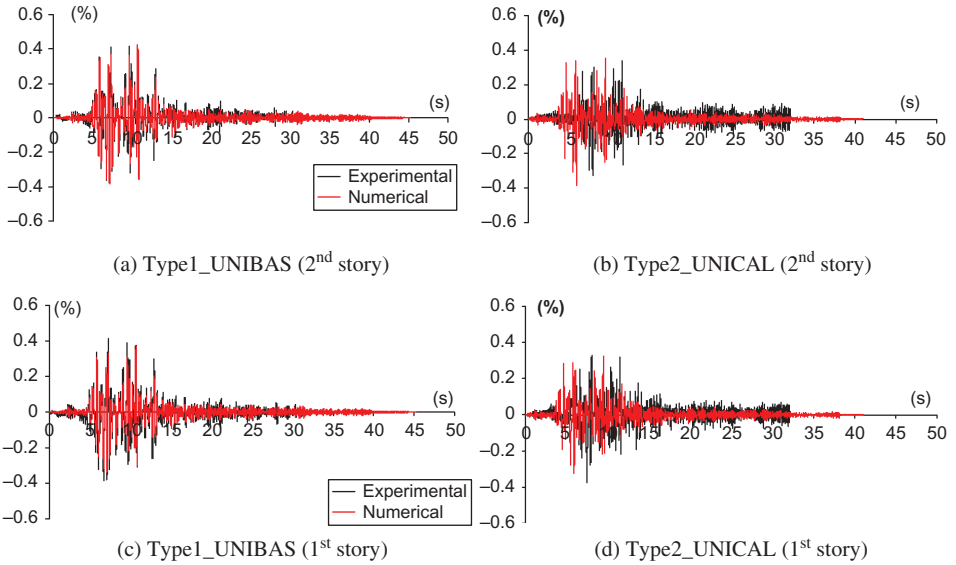

FIGURE 16 Experimental and numerical results for inter-story drifts: accelerogram 196@ 100% (color figure available online).

structure. More specifically, the adoption of Type2_UNICAL devices led to drifts less than the corresponding ones experienced using Type1_UNIBAS devices. But, as expected, the maximum load reached by the device was greater for Type2_UNICAL; then, this led to higher values of the floor accelerations. Moreover, the HYDs showed a considerable damping capacity, for both the design solutions, and a stable hysteretic behaviour, for a large number of load cycles.

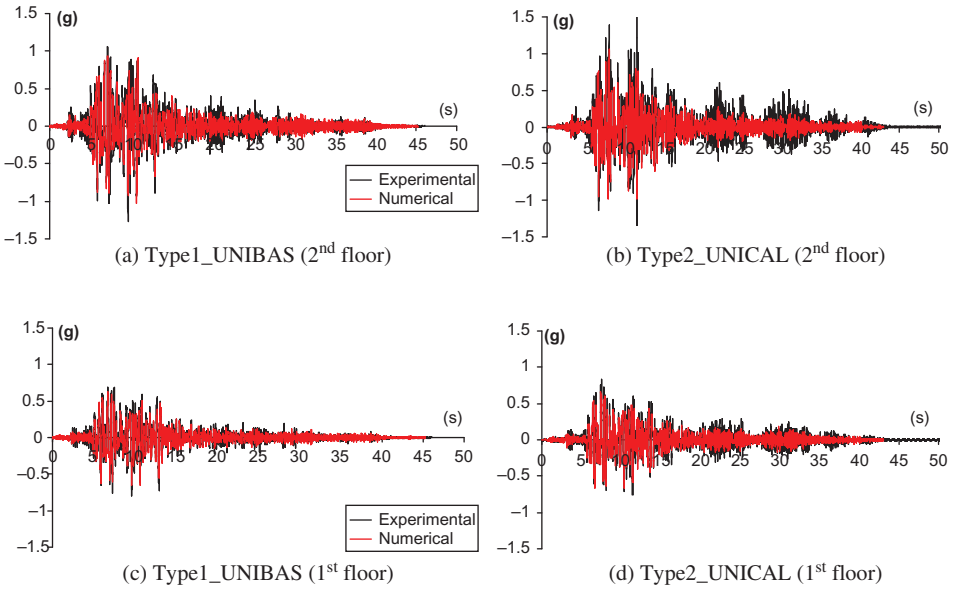

(a) Type1_UNIBAS (2nd floor) (b) Type2_UNICAL (2nd floor)

(c) Type1_UNIBAS (1st floor) (d) Type2_UNICAL (1st floor)

FIGURE 17 Experimental and numerical results for floor accelerations: accelerogram 196@100% (color figure available online).

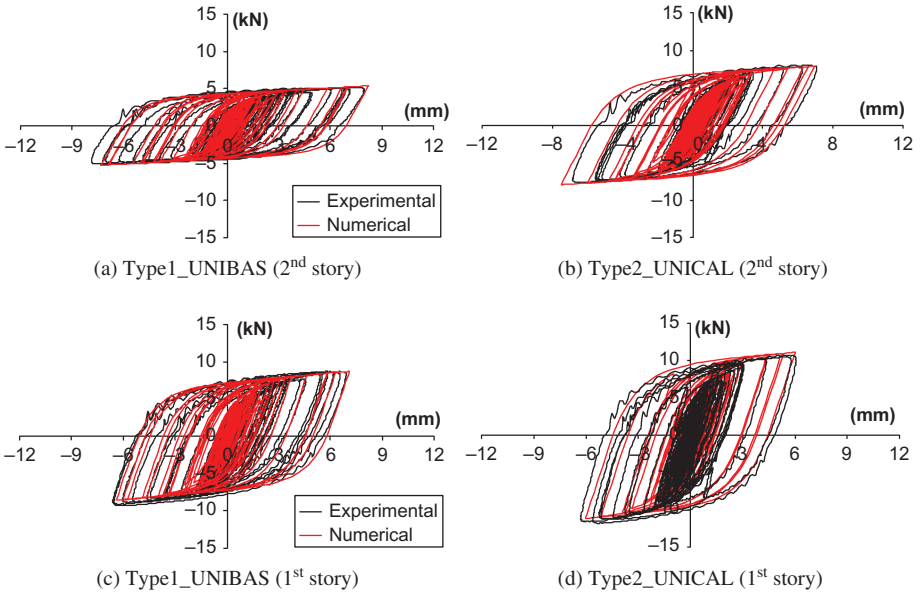

(a) Type1_UNIBAS (2nd story) (b) Type2_UNICAL (2nd story)

(c) Type1_UNIBAS (1st story) (d) Type2_UNICAL (1st story)

FIGURE 18 Comparison between experimental and numerical force-displacement cyclic laws: accelerogram 196@ 100% (color figure available online).

Finally, experimental outcomes proved the robustness of the EDB systems in well-controlled seismic vibrations even for significant changes of the ductility factor and yield strength of the elastic-plastic devices, like those corresponding to Type1_UNIBAS and Type2_UNICAL design solutions compared in the present work. This property is essential because real values of the above-mentioned mechanical properties can be quite different

from the design values due to industrial standardization in the production of the devices and/or some their damage suffered during previous earthquakes.

Acknowledgments

The present work was financed by R.E.L.U.I.S. (Italian network of university laboratories of earthquake engineering), within the "D.P.C. – R.E.L.U.I.S. Project 11/07/2005 (item 540) research line no. 7".

References

Antonacci, E., De Stefano, A., Gattulli, V., Lepidi, M., and Matta, E. [2011] "Comparative study of vibration-based parametric identification techniques for a three-dimensional frame structure," *Structural Control and Health Monitoring*, Wiley Online Library.

Bertero, V. V. [2002] " Innovative approaches to earthquake engineering," ed. G. Oliveto, (University of Catania (Italy),WIT Press), pp, 1–84.

Bouc, R. [1967] " Forced vibration of mechanical systems with hysteresis," *Proc. of the 4th International Conference on Nonlinear Oscillation*, Prague, Czechoslovakia.

Christopoulos, C. and Filiatrault, A. [2006] "Principles of passive supplemental damping and seismic isolation," IUSS Press, Istituto Universitario di Studi Superiori di Pavia, Pavia, Italy.

Ciampi, V. [1989] "Un sistema di controventi dissipative per strutture antisismiche in acciaio," *International Meeting on Base Isolation and Passive Energy Dissipation*, Assisi, Italy, pp, 17.01–17.16.

Ciampi, V. [1993] "Development of passive energy dissipation techniques for buildings," *International Post-SMIRT Conference Seminar on Seismic Isolation, Energy Dissipation and Control of Vibrations of Structures*, pp. 495–510.

Di Cesare, A., Ponzo, F. C., Auletta, G., and Gilio A. [2011] "Behaviour factor of concrete structures with hysteretic energy dissipating bracing system," *Proc. of the XIV ANIDIS L'Ingegneria Sismica in Italia*, Bari, Italy.

CSI [2004] *SAP2000: Static and Dynamic Finite Element Analysis of Structures*, Computers and Structures, Inc,, Berkeley, CA.

De Stefano, A., Matta, E., and Quattrone, A. [2008] "Dynamic identification and model-updating of the JETPACS prototype," *DPC-RELUIS Research Project No. 7*, JETPACS Report No. 4.

Dolce, M., Filardi, B., Marnetto, R., and Nigro, D. [1996], "Experimental tests and applications of a new biaxial elasto-plastic device for the passive control of structures," *Proc. of the 4th World Congress on Joint Sealants and Bearing Systems for Concrete Structures*, Sacramento, CA.

Dolce, M., Ponzo, F.C., Di Cesare, A., Ditommaso, R., Moroni, C., Nigro, D., Serino, G., Sorace, S., Gattulli, V., Occhiuzzi, A., Vulcano, A., and Foti, D. [2008] "JET-PACS project: Joint Experimental Testing on Passive and Semiactive Control Systems, *Proc. of the 14th World Conference on Earthquake Engineering*, Beijing, China, paper No. 183.

Eurocode 8 [2003] *Design of Structures for Earthquake Resistance - Part 1: General Rules, Seismic Actions and Rules for Buildings*, C.E.N., European Committee for Standardization.

European Commission for Community Research. European Strong Motion Database (on-line), http:// www.isesd.cv.ic. ac.uk/ESD.

FEMA-ASCE 356 [2000] *Prestandard and Commentary for the Seismic Rehabilitation of Buildings*. Federal Emergency Management Agency and American Society of Civil Engineering, Washington, D.C.

Gattulli, V., Lepidi, M., and Potenza, F. [2007] "Identification of analytical and finite element models for the JETPACS three-dimensional frame," *DPC-RELUIS Research Project No. 7*, JETPACS Report No. 2.

Iervolino, I., Maddaloni, G., and Cosenza, E. [2008] "Eurocode 8 compliant real record sets for seismic analysis of structures," *Journal of Structural Engineering* **12**, 54–90.

Kelly, J. M., Skinner, R. I., and Heine, A. J. [1972] "Mechanisms of energy absorption in special device for use in earthquake resistant structures," *Bulletin of the New Zealand Society of Earthquake Engineering* **5**(3), 63–88.

Kim, J. and Choi, H. [2006] "Displacement-based design of supplemental dampers for seismic retrofit of a framed structure," *Journal of Structural Engineering* **132**(6), 873–883.

Kim, J., Choi, H., and Min, K. W. [2003] "Performance-based design of added viscous dampers using capacity spectrum method," *Journal of Earthquake Engineering* 7(1), 1–24.

Martìnez-Rueda, J. E. [2002] "On the evolution of energy dissipation devices for seismic design," *Earthquake Spectra* **18**(2), 309–346.

Mazza, F. and Vulcano, A. [2008] "Displacement-based seismic design procedure for framed buildings with dissipative braces. (a) Part I: Theoretical formulation; (b) Part II: Numerical results," *2008 Seismic Engineering International Conference Commemorating the 1908 Messina and Reggio Calabria Earthquake (MERCEA08)*, Reggio Calabria (Italy), American Institute of Physics Conference Proceedings, Vol. 1020 (part two). Q13

NTC [2008] "Italian Technical Code for Constructions (in Italian)," *DM 14 gennaio 2008*, Rome, Italy.

Ponzo, F. C., Cardone, D., Di Cesare, A., Moroni, C., Nigro, D., and Vigoriti, G. [2007a] "Dynamic tests on JETPACS steel frame: experimental model set up," *DPC-RELUIS Research Project No. 7*, JETPACS Report No. 3. Q14

Ponzo, F. C., Dolce, M., Di Cesare A, Vigoriti, G., and Arleo, G. [2007b] "A design procedure for energy dissipating displacement-dependent bracing system for r/c buildings," *Proc. of the 10th World Conference on Seismic Isolation, Energy Dissipation and Active Vibrations Control of Structures*, Istanbul (Turkey). Q15

Ponzo, F. C. and Di Cesare, A. [2009] "Numerical and experimental assessment of the robustness of a seismic upgrading technique for framed buildings based on hysteretic dissipating devices," *Proc. of the 11th World Conference on Seismic Isolation, Energy Dissipation and Active Vibration Control of Structures*, Guangzhou (China). Q16

Serino, G., Chandrasekaran, S., Marsico, M. R., and Spizzuoco, M. [2008] "Descriptions and analytical modelling of the Jetpacs prototype steel frame," *DPC-RELUIS Research Project No. 7*, JETPACS Report No. 1. Q17

Soong, T. T. and Dargush, G. F. [1997] *Passive Energy Dissipation Systems in Structural Engineering*, John Wiley & Sons Ltd, Chichester, UK.

Tsai, K. C., Chen, H. W., Hong, C. P., and Su, Y. F. [1993] "Design of steel triangular plate energy absorbers for seismic-resistant construction," *Earthquake Spectra* **9**(3), 505–528.

Vulcano, A. and Mazza, F. [2002] "A simplified procedure for the aseismic design of framed buildings with dissipative braces," *Proc. of the 12th European Conference on Earthquake Engineering*, London, Paper No 735.

Wen, Y. K. [1976] "Method of random vibration of hysteretic systems," *Journal of Engineering Mechanics* **102**, 249–263.

Whittaker, A. S., Bertero, V. V., Thompson, C. L,. and Alonso, L. J. [1991] "Seismic testing of steel plate energy dissipation devices," *Earthquake Spectra* **7**(4), 563–604.